Benajes Calvo, JV.; Payri Marín, R.; Bardi, M.; Marti-Aldaravi, P. (2013). Experimental characterization of diesel ignition and lift-off length using a single-hole ECN injector. Applied Thermal Engineering. 58(1-2):554-563. doi:10.1016/j.applthermaleng.2013.04.044.

Experimental characterization of Diesel ignition and Lift-off length using a single-hole ECN injector

Jesús Benajes[a], Raúl Payri[*,a], Michele Bardi[a], Pedro Martí-Aldaraví[a]
[a] CMT-Motores Térmicos, Universitat Politècnica de València, Camino de Vera s/n, 46022 Valencia, Spain

Abstract

In this work, lift-off length and ignition delay have been measured via chemiluminiscence techniques in a wide range of conditions for a single-hole injector from the Engine Combustion Network (ECN) dataset and using a single component fuel (n-dodecane). In addition, Schlieren technique was used to characterize the ignition event using a new developed post-processing methodology capable of characterizing the “disappearance” phenomenon linked to the start of cool flames. Experiments have been carried out in a novel constant-pressure flow facility able of reproducing engine-like thermodynamic conditions. Results show that oxygen concentration seems to have a negligible impact on the start of cool flames. Empirical correlations have been obtained for the three measured parameters and they manifest similar trends of other previously published correlations for lift-off length and second stage ignition. These correlations also underline that the effect of oxygen concentration and ambient density is caught differently by chemiluminiscence and Schlieren techniques, even though the absolute value of the measurements remains close.

Keywords:
Diesel injection; ECN; Cool Flames; Ignition; Lift-off Length; Schlieren;

Highlights:

- Ignition delay and *LOL* of an ECN injector are measured with ECN standard diagnostics.
- New processing is developed for Schlieren images to obtain first/second stage ignition.
- A sweep of pressure, density, temperature and oxygen concentration is performed.
- A statistical analysis is done to provide an analytical description of the results.

Nomenclature

A, a, b, c, d: parameters adjusted in the statistical analysis

Δp_{nozz}: pressure drop through the nozzle orifice

ASOI: after the start of injection

CPF: constant-pressure flow (facility)

cwl: center wave length

CVP: constant volume pre-burn (facility)

[*] Corresponding author. e-mail: rpayri@mot.upv.es. Phone number: +34 - 963879658

APPLIED THERMAL ENGINEERING; Volume: 58; Issue: 1-2; Pages: 554-563;
DOI: 10.1016/j.applthermaleng.2013.04.044; Published: SEP 2013

D_0: nozzle orifice outlet diameter
k-factor: nozzle orifice conicity factor, defined as $k\text{-}factor = 100 \cdot (D_i - D_o)/L$.
LOL: lift-off length
$O_2\%$: ambient oxygen concentration
p_{amb}: ambient pressure
p_{rail}: rail pressure
SSI: second stage ignition
SoCF: start of cool flames
T_{amb}: ambient temperature
t: time
u_{th}: theoretical velocity of the fuel at the orifice outlet
UV: ultra violet
v_i: instantaneous spray velocity
ρ_{amb}: ambient density
ρ_{fuel}: fuel density

1. Introduction

Air-fuel mixing, evaporation and combustion processes control is the key to reduce pollutants and improve the efficiency of direct injection Diesel engines [1], [2]. Since decades, engine researchers have been trying to understand the basis of these processes from different points of view: theoretical, experimental and computational. Computational tools, such as computational fluid dynamics (CFD) simulations, have proved their great potential [2], [3] and are growing and improving every day as proved by the use of new and models able to provide more detailed data such Deatached Eddy Simulation [4] or Large Eddy Simulation [5]. Still, these models are not completely predictive and experimental data are necessary at least for validation, but also to correctly define the boundary conditions of the problem.
Because all the relevant variables are accessible in CFD models, including local and transient fields, experimental methodologies and database need to be enhanced with more quantitative, accurate and reliable information. The Engine Combustion Network (ECN) [6] started an international collaboration in order to provide high quality data and consistent results to modelers. The work of the group lays on several coordinated efforts in the Diesel research field: the complete definition of a standard reference condition, the use of nominal identical injectors (donated by Bosch to the ECN) and the organic cross check of the data obtained by different facilities and through different techniques. Among the guidelines chosen recently by the group there is also the introduction of standard experimental diagnostics [6], [7] in order to create coherent databases between the institutions and to reduce the uncertainties when the data from different facilities are compared. On the same spirit, a table of parametric variations in the boundary conditions has been introduced including variations in ambient temperature, ambient density, oxygen concentration and injection pressure.

APPLIED THERMAL ENGINEERING; Volume: 58; Issue: 1-2; Pages: 554-563;
DOI: 10.1016/j.applthermaleng.2013.04.044; Published: SEP 2013

In the present work a novel constant-pressure flow facility (CPF) [8] able to reach 15 MPa ambient pressure and 1000 K ambient temperature, has been employed to carry out experimental studies of the combustion process, concretely the characterization of the ignition delay and the lift-off length at Diesel-like conditions following the ECN recommendations. Therefore, the whole range of suggested parametric variations has been studied employing the standard experimental methodologies:

- Broadband chemiluminescence technique, to measure ignition delay [7], [10]
- OH* chemiluminescence to measure steady *LOL* [9], [11]

Both techniques are deeply described in the literature. Moreover, a special effort has been made to study the spray disappearance phenomenon observed when a Schlieren setup is used to study a reacting Diesel spray [7], [12]. A novel processing method has been applied and the results obtained allow to clearly distinguishing the onset of cool flames and the ignition delay (or second stage ignition).

Thanks to the broad range of the conditions tested, the results have been analyzed statistically and empirical correlations have been obtained. In this last part of the work the results have been compared with other works in the literature in order to remark the reliability and the high quality of the experimental data provided.

2. Material and Methods

2.1 The constant-pressure flow facility

A novel constant-pressure flow test chamber capable of mimicking the in-cylinder thermodynamic conditions of a Diesel engine at the time of injection was used. Following the convention presented by Baert et al. [8] the test rig is classified as a constant-pressure flow (CPF) facility because the Diesel-like conditions are reached by means of a continuous flow of high temperature high pressure gas through the test chamber. Compared to other facilities this test rig has the unique feature of obtaining nearly quiescent and steady thermodynamic conditions within the chamber, providing thus an important reduction in the time required for the tests. In order to measure correctly the temperature at the conditions tested, radiation heat transfer should be taken into account [13].

In Figure 1 a sketch of the layout of the facility is provided. The boundary conditions have been deeply characterized in [14] and a complete description of the facility is given in [15], [16].

2.2 The injection system

The injection system employed consists of commercial available components: a high pressure volumetric Bosch CP3 pump driven by an electric motor; a common rail with pressure regulator controlled by a PID system; and a special injector holder which is used to keep constant the injector tip temperature [16] though the whole test matrix.

APPLIED THERMAL ENGINEERING; Volume: 58; Issue: 1-2; Pages: 554-563;
DOI: 10.1016/j.applthermaleng.2013.04.044; Published: SEP 2013

The injector employed, based on second generation Common-Rail, is part of the ECN injector dataset (ref: #210675 [6]). The injector features a single-hole axial nozzle enabling the advantage to focus on the fundamental behavior of the spray eliminating both the effects and the uncertainties related to the temperature boundary layer close to the walls and the spray-spray interaction. Moreover, ECN injectors' internal geometry and hydraulic behavior has been deeply characterized and the data are available in [17].
Following the ECN philosophy, in order to enable the comparison with a CFD simulation, a single-component fuel has been employed (n-dodecane): in fact a wide amount of data about this fuel can be found in the literature [18].

2.3 The test matrix

The test matrix is summarized in Table 1. It includes the Spray A operating conditions (T_{amb} = 900 K, ρ_{amb} = 22.8 kg/m^3, p_{rail} = 150 MPa, O_2 = 15% (vol.)) and variations of the main variables (oxygen concentration, ambient temperature, ambient density and injection pressure) as defined by ECN Working Group. The large range of values tested also allow to build statistically reliable empirical relationships and to compare them with theoretical or previously obtained by other authors' results.

Table 1. Test conditions summary.

Parameter	Values	Units
Fuel	n-dodecane	-
Orifice diameter (D_o)	0.089	mm
k-factor[a]	2.1	-
Energizing time	4000	μs
Tip temperature	390	K
Gas density (ρ_a)	7.6, 15.2, 22.8	kg/m^3
Gas temperature (T_{amb})	750, 800, 850, 900	K
Injection pressure (p_{rail})	300, 500, 750, 1000, 1250, 1500	MPa
Oxygen concentration (O_2%)	13, 15, 21	% (vol.)

[a] *k-factor definition is given by Macian et al. [19].*

2.4 Optical techniques and processing methods

2.4.1 Diesel ignition study

Diesel ignition is strictly linked with chemiluminescence light emissions that take place during the combustion [20]. Dec and Coy [21] demonstrated that the two main phases of the Diesel ignition, onset of cool flames and second stage ignition, can be characterized by imaging the natural emissions of two radicals, respectively CH* and OH*. During the last years, several authors used intensified cameras fitted with interferometric filters to isolate the chemiluminescence emissions from CH* (at 430 nm) and OH* (at 310 nm) [22], [23]. Despite the important results shown by these techniques, two drawbacks of this approach should be highlighted:

- The best reliability in terms of sensitivity is given by the single shot ICCD cameras, which allow capturing only one image per injection event. Therefore, the time required

for the characterization of a time dependent event (e.g. Diesel ignition) is significantly increased. Furthermore transient events during one injection cannot be captured (e.g. vortex development).

- When measuring the very weak emissions of CH* the sensitivity of the setup is fundamental, and even an intensified camera may not be able to catch the very beginning of cool flames [16]. Moreover, in the case CH* emissions are detected it is not straight forward to know that the setup is catching the emissions from the beginning.

In order to overcome these problems alternative techniques have been used in this work: broadband chemiluminescence [7], [10] and the Schlieren imaging [12], [24] both implementable with the use of fast cameras.

Before going further in the description of the techniques employed, it is convenient to define the two parameters characterized in the ignition delay study and the relationship between them.

- *Start of cool flames (SoCF):* time elapsed between the start of injection and the first insight of onset of chemical reactions.
- *Start of high temperature reactions or second stage ignition (SSI):* this parameter normally known also as ignition delay is the time, referred to the start of injection, at which the high temperature release reactions start.

Cool flames depend mainly on chemistry scale. There is a negative temperature gradient region and a thermal preparation region before SSI is initiated. To understand SSI, the thermal preparation region is more important to consider because during this period reactions with formaldehyde are consumed and hydrogen peroxide decomposes to produce OH radicals, which subsequently react and initiate SSI. On the other hand, SSI also depends on mixing (turbulent scale) that subsequently depends on injection pressure, ambient density, local oxygen concentration and turbulence level in the combustion chamber.

2.4.2 Broadband Chemiluminescence

Broadband chemiluminescence technique to study ignition delay was introduced and validated by Lillo et al. [10]. Following their idea, a standard processing has been defined and it is described next. As shown in Figure 2, where the maximum intensity (counts) computed in the area of interest (roughly, in the *LOL* region) is plotted, the intensity related to the cool flames is orders of magnitude lower than the one of high temperature chemiluminescence, and the latter stabilizes at a certain level also defined as leveling-off level. The leveling-off level could thus be used as a reference for calculating the SSI threshold, that as per ECN guidelines is fixed at 50%. Even if an insight of cool flames can be detected with this technique the measurement performed falls in the same limitation of the CH* imaging with intensified camera: the very week signal captured makes it impossible to state if the setup is catching the very beginning of the process. Details of the optical setup are listed in Table 2.

Table 2. Details of the optical setup used in the study.

	Broadband chemilum.	Schlieren Imaging	OH* chemilum.
Camera	Phantom - V12	Photron SA-5	Andor - Istar
Sensor Type	CMOS	CMOS	ICCD
Lens	100 mm	50 mm	100 mm - U.V.
Diaphragm	-	4 mm	-
Filter	<600 nm	-	310 cwl ± 5
Frame Rate	20 kfps	50 kfps	1 frame/injection
Shutter time	48 μs	4 μs	3 ms (from 2 to 5 ms ASOI)
Repetitions	8	8	15
Pixmm	7.25	5.26	5.85

2.4.3 Schlieren imaging

Schlieren imaging is a valuable technique to identify refractive index gradients in transparent media [24]. For vaporizing Diesel [25], [26] but also gasoline [27] sprays, this technique shows the boundary between vaporized fuel and ambient gases because (1) refractive index differences exist between the fuel and ambient gases and (2) density gradients are created in mixture as the vaporized fuel spray cools the mixture. The good temporal resolution of this technique allows characterizing the spray even for a fast response injectors [28].

Pickett et al. [12], using a Schlieren setup, observed that cool flames onset can be appreciated as a temporal disappearance of the spray in the tip region. As explained by Pickett et al. [12], this phenomenon is related to the changes in chemical composition and temperature of the mixture that take place in this early phase of the ignition. The refractive index of the mixture changes and for a transient period is very close to the one of the surrounding gas, becoming then invisible to the Schlieren setup. Bardi et al. [7] observed consistently this phenomenon in different facilities and compared the different experiments basing on the measured spray penetration.

Figure 3 presents image sequences captured by the two optical setups for a sample test condition highlighting the features of the ignition detected by both techniques. In the Schlieren imaging, at about 420 μs ASOI the spray tip starts getting transparent (even if it is still visible) and disappears completely at 460 μs ASOI as a consequence of the onset of cool flames. At about 620 μs ASOI the spray tip is still transparent and the first signal is captured by the broadband chemiluminescence setup: this is considered the last, most luminous phase of the cool flames. In the following image (660 μs ASOI) the chemiluminescence signal significantly increases together with the refractive index gradients in the spray (the spray tip re-appear in the Schlieren image): this is considered the instant when the second stage ignition takes place. Suddenly after the *SSI*, soot incandescence becomes the dominant light emitting source, causing the broadband signal to get stronger and saturate the camera sensor. On the other

hand, due to the important temperature gradient occurring in the diffusive phase of the combustion and to the soot absorption, the spray tip in the Schlieren images becomes darker. In order to analyze in a factual way the disappearance phenomenon observed through the Schlieren setup and to compare the event under different test conditions, a special image processing has been developed:

- *Background correction*: shadowgraph imaging under high temperature conditions is characterized by background structures caused by the gas temperature/density in-homogeneities. These structures cannot be considered steady during the injection event. On the other hand, this movement is slow compared to spray velocities, so the structures can be considered steady between two consecutive images. For this reason, a common way to analyze Schlieren images is a derivative analysis, where the spray detection basis on the subtraction of one image to the following one. In this case, being the focus of the processing to observe the transparency effect in the spray it would not be convenient to subtract the previous image because the core of the spray would be subtracted to itself, and much information would be lost. A different strategy was therefore developed for the background subtraction. To characterized the image I_i, composite background image $I_{bg,i}$ is subtracted, that is obtained combining different images: $I_{bg,i}$ is composed by the area that in the image I_{i-1} was not filled by the spray; the remaining area of I_{i-1} is filled by the pixels that in the image I_{i-2} were not occupied by spray, and so on. In other words the pixels of the background are chosen from the last image in which they were not part of the spray.
- *Segmentation criterion:* spray boundaries are determined binarizing the image following the approach described by Siebers [29]. The binarization threshold is defined as the 5% of the dynamic range of each background corrected image.
- *Total intensity calculation (y)*: the global Schlieren effect of the spray is evaluated computing the total intensity of the corrected image, in other words, the counts of each pixel of the corrected image are summed to have a single value.
- *Total intensity increment (Δy):* finally, Δy is defined as the increment of the parameter y between two following images.

Analyzing the parameter Δy the transparency phenomenon is evaluated globally, considering also the changes occurring not only along the border but also within the core of the spray.
In Figure 4 (left), a time plot of the parameter y is presented: as the injection event advances in time and the spray grows larger, the total intensity increases. At the time cool flames start, the spray gets transparent and the total intensity trend changes. Afterward, as the spray tip appears again in the Schlieren image, the total intensity restarts growing as a consequence of the second stage ignition. The two changes in the slope of the curve correspond to the two peaks observed in Figure 4 (right), where the total intensity increment is plotted. Observing Figure 4 (right), three main conclusions can be laid: i) the cool flame effect is quite robust to the Schlieren setup since it is observed at different diaphragm apertures; however, the comparison suggests that when the diaphragm aperture is reduced [24] the peaks appear more prominent

APPLIED THERMAL ENGINEERING; Volume: 58; Issue: 1-2; Pages: 554-563;
DOI: 10.1016/j.applthermaleng.2013.04.044; Published: SEP 2013

and therefore their detection is easier and the diaphragm aperture chosen for the entire test matrix is 4 mm; ii) at a certain point an evident deviation can be observed between the reacting/non-reacting case; the interval between this instant and the start of injection will be named *SoCF* (Start of Cool Flames) (c.f. Figure 4 (right)); and iii) the second stage ignition is associated with a well-defined local maximum in the total intensity increment curve; the relationship between this event and the *SSI* obtained in broadband chemiluminescence will be discussed in the next section. Finally, in Figure 4 (left and right), a sample of the shot-to-shot standard deviation of the curves is represented by the light blue area and it indicates that the measurement has a very good repeatability providing thus precise measurements.

2.4.4 Lift-off length

The lift-off length (LOL) was measured capturing the signal from OH* chemiluminescence following the ECN standard methodology [6], [9]. An ICCD camera (Andor I-star) fitted with a 100 mm f/2.8 UV lens and a 310±5 nm interferometric filter was used with a constant intensifier gating time widow included between 2.0 and 5.0 ms ASOI: in this way the steady part of the injection was averaged along the injection event and the shot-to-shot deviation was reduced. Once images are captured, the post-processing follows the approach presented by Siebers and Higgins [9]: after filtering the image with a 3x3 pixel mean filter, two intensity profiles are obtained calculating the maximum intensity for each axial position in the upper and lower half of the image (Figure 5 left). The lift-off length was determined by finding the distances between the injector tip and the first axial locations above and below the spray centerline with intensity greater than 50% of the intensity peak shown in Figure 5 left-bottom. The average of these two axial distances is defined as the lift-off length. Considering the dependence of the peak value on ambient/injection boundary conditions (Figure 5 right), the lift-off length threshold was obtained calculating the peak value for each combination of them following the approach below:

- For each condition tested, all the repetition-images were used to obtain a single average-image;
- A characteristic intensity profile was extracted averaging the upper and lower intensity profiles (see above) of the average image and finally, the threshold was scaled to the 50% of the peak observed in this curve.

In Figure 5 left-top, the colored dashed lines indicate the *LOL* calculated for a sample image scaling the threshold to a different percentage of the peak: the separation between the *LOL* values obtained underlines how the threshold definition and the method used to compute it have an important effect on the final result.

3. Results

In order to give to this section a linear organization, authors preferred to start discussing the results from comparison between Schlieren and broadband chemiluminescence experiments, and concluding with the *LOL* analysis.

APPLIED THERMAL ENGINEERING; Volume: 58; Issue: 1-2; Pages: 554-563;
DOI: 10.1016/j.applthermaleng.2013.04.044; Published: SEP 2013

3.1 Schlieren/broadband chemiluminescence images

When the total intensity increment curves under different test conditions are compared on the same axis (Figure 6 and Figure 7) several considerations can be drawn:

- In all the conditions tested, always a clear deviation between the reacting and non-reacting curves occurs at a certain point of the injection. This allows identifying the start of the transparency phenomenon and thus the *SoCF*.
- The local maximum that is following the transparency phenomenon is always in good agreement with the second stage ignition delay obtained via broad-band chemiluminescence (dashed vertical lines). This observation is consistent through most of the conditions tested, suggesting an interesting potential of the Schlieren technique for the evaluation of the *SSI*. Therefore, the time corresponding to this peak is recorded and then used for a further and more general comparison. This parameter will be recalled as *SSI Schlieren*.
- When ambient temperature is decreased a third peak appears as a local maximum right before the minimum mentioned above (Figure 6 left), meaning that the spray gets darker for a short time right before the transparency phenomenon. This effect is possibly related to the different chemical reactions that are taking place at low ambient temperature [30], [31] and that are affecting the mixture refractive index evolution.

In Figure 8 and Figure 9 the parameters *SoCF* and *SSI* are plotted together for comparison. In these figures it is possible to appreciate the effect that the test conditions have on these parameters and on the related time-dwell. While the effect of oxygen concentration and ambient temperature can be chemically explained (typically higher oxygen concentration and ambient temperature accelerate oxidation reactions as expected theoretically [32] and observed experimentally by other authors [33], [34]) the effect of ambient density and injection pressure is related to fuel-air mixing dynamics. At higher ambient density the spray spreading angle increases significantly [35]: in this condition the volume of air entrained in the spray is higher (and denser), causing therefore a faster heating of the fuel mixture. On the other hand when injection pressure is increased the spray penetrates and mixes faster [36] leading the fuel to reach the ignition condition earlier. These considerations apply to both parameters, *SoCF* and *SSI*.

Comparing the effect that the variations in test conditions have on *SoCF* and *SSI*, it appears that while ambient temperature and injection pressure are substantially reducing both parameters in the same proportion, ambient density has a reduced effect and oxygen concentration barely affects *SoCF*, both increasing substantially the *SoCF-SSI* time dwell. This phenomenon will be further examined in the discussion section.

Figures 8 and 9 also show that *SSI* from Schlieren well matches the *SSI* value obtained via broadband chemiluminescence in the whole bench of conditions tested. However, differences occasionally appear between the two measurements, but in most of the cases these differences seem to be caused more by boundary condition uncertainties and shot-to-shot dispersion rather

APPLIED THERMAL ENGINEERING; Volume: 58; Issue: 1-2; Pages: 554-563;
DOI: 10.1016/j.applthermaleng.2013.04.044; Published: SEP 2013

than to the technique employed. A different consideration should be done for the results at low ambient gas density and low ambient temperature. At low ambient density the Schlieren technique clearly over-predicts the SSI: even if it is not easy to demonstrate theoretically, this fact is not so surprising. As explained before, Schlieren imaging detects the refractive index gradients along the test section and therefore the whole disappearing/re-appearing phenomenon has to be related to difference between the (average) refractive index of the spray and of the surrounding gas. Being the ambient density the main driver for air refractive index, when this parameter is substantially reduced (e.g. from 22.8 to 7.6 kg/m^3) the physical threshold for the disappearing phenomenon is somehow changed, and therefore the related measurements might be affected. At low ambient temperature, Schlieren technique seems to overestimate SSI: the different intermediate products generated lead to different refractive index evolution (see LOL results in the next section) and again the related measurements might be affected.
Finally it is important to point out that the standard deviation of the *SSI* measured via chemiluminescence and via Schlieren is in all the cases lower than the 5% of the measurement indicating a very good repeatability of the tests and of the measurement.

3.2 Lift-off length results

The lift-off length obtained under different test conditions is plotted in Figure 10 and 11. The results reflect what was already observed in other works [9], [34]: lift-off length decreases when oxygen concentration, ambient temperature and ambient density increase, and increases with injection pressure. The very low standard deviation obtained (always lower than 7% of the measured value), underlines the high repeatability of the measurements guaranteed by the long exposure time of the camera that integrates all the fluctuations characteristics of the spray turbulences, and by the steady test conditions of the test rig. The effects of the test conditions on the lift-off length will be better quantified in the next section through a statistical analysis.

4. Discussion

The broad range of conditions tested gives a solid base to perform a statistical analysis and increase the reliability of the results. A least-square regression has been performed to have an analytical description of the relationship between the test conditions and the measurements performed.
The equations used have been chosen depending on the parameter analyzed. On one hand, *SSI* and *SoCF*, which are directly related to the combustion chemistry, are fitted to an Arrhenius type: Equation (1). On the other hand, *LOL* is strongly linked to the spray development and therefore an exponential equation is preferred: Equation (2). Moreover, in other works [15], [34] the same equations have been chosen to perform a similar analysis and therefore the new results obtained in the two cases can be compared.

APPLIED THERMAL ENGINEERING; Volume: 58; Issue: 1-2; Pages: 554-563;
DOI: 10.1016/j.applthermaleng.2013.04.044; Published: SEP 2013

$$ID \propto \exp\left(\frac{A}{T_{amb}}\right) \cdot \rho_{amb}^{a} \cdot \Delta p_{nozz}^{b} \cdot O_{2\%}^{c} \quad (1)$$

$$LOL \propto T_{amb}^{a} \cdot \rho_{amb}^{b} \cdot u_{th}^{c} \cdot O_{2\%}^{d} \quad (2)$$

Where Δp_{nozz} is the pressure drop through the nozzle orifice approximated to $p_{rail} - p_{amb}$, and u_{th} the theoretical velocity of the fuel at the orifice outlet obtained as:

$$u_{th} = \sqrt{2\frac{\Delta p_{nozz}}{\rho_{fuel}}} \quad (3)$$

being ρ_{fuel} the density of the fuel. Table 3 shows part of the results from the statistical analysis performed. Concerning the *SSI* obtained by the broadband chemiluminescence, results show relatively good agreement with the results from Pickett et al. [34]. Although small differences appear, the general trend is very close and the high R^2 found is proving the good precision of the tests and the reliability of the results. Moreover, the constant *A*, related to the effect of the ambient temperature, is affected by the fuel employed: Pickett et al. [34] used DR2 reference fuel while in the present work the fuel used is pure n-dodecane and therefore some difference in *A* should be expected.

Table 3. Coefficients obtained from the regression of Equation (1) to the experimental data for SSI and SoCF. Coefficients obtained by Pickett et al. [34] are reported for reference.

	A	***a***	***b***	***c***	***R^2 [%]***
SSI - Picket et al. [34]	6534	-0.96	-	-1	-
SSI - Chemiluminiscence	7216	-1.25	-0.09	-0.93	98.0
SSI - Schlieren	7523	-1.35	-0.09	-0.51	97.9
SoCF	8312	-0.7	-0.2	-0.05	97.9

When the *SSI* obtained via Schlieren methodology is analyzed, it is proved that the technique is consistent when ambient temperature and injection pressure are changed, but the measurement loses its precision when ambient density or oxygen concentration are varied. However even if the coefficients obtained for oxygen concentration and ambient density are quite different, it has to be underlined that the absolute value of the measurement is very close to the one obtained via chemiluminescence (the maximum relative difference is 13%, including uncertainties in test conditions and shot-to-shot repeatability) and therefore the potential of the methodology is confirmed.

Analyzing the effect of the test parameters on *SoCF* two relevant facts have to be remarked:

- The high R^2 underlines that the transparency phenomenon is highly reproducible and it can be precisely determined in all the range of tested conditions.
- *SoCF*, when compared to the *SSI*, is only slightly affected by oxygen concentration (as shown in Figure 9) and is more sensitive to the effect of injection pressure. This means

APPLIED THERMAL ENGINEERING; Volume: 58; Issue: 1-2; Pages: 554-563;
DOI: 10.1016/j.applthermaleng.2013.04.044; Published: SEP 2013

that with respect to *SSI,* cool flames timing is more related to the mixing process and not only to chemistry as first thought.

The statistical study is concluded analyzing the *LOL* measurements using Equation (2). It is summarized in Table 4. The number of conditions tested and the high value of R^2 obtained allows having a very accurate analytical description of the data obtained over a wide range of test conditions. When compared to coefficients found by Pickett et al. [34] an important agreement is still found concerning the effect of ambient temperature, ambient density and oxygen concentration. However, an important difference has been observed in the effect that injection pressure has on *LOL*.

Table 4. Coefficients obtained from the regression of Equation (2) to the experimental data for LOL. Coefficients obtained by Pickett et al. [34] and Payri et al. [15] are reported for reference.

	a	***b***	***c***	***d***	***R^2 [%]***
Picket et al. [34]	-3.74	-0.85	1	-1	-
Payri et al. [15]	-3.97	-0.93	0.52	-	-
Experimental data	-3.89	-1	0.54	-1	99.5
Experimental data (including T_{amb} = 750 K)	-5.10	-1.14	0.31	-0.86	98.0

Coefficients presented in the third row of Table 4 have been obtained excluding the 750 K data. If the same fitting is done including those data (fourth row) coefficients widely differ from those obtained by other authors. This is because at low ambient temperature balances along chemistry mechanisms in the oxidation process vary, changing the velocity of the reactions and the amount of the intermediate products that are generated [30], [31]. Thus, a different correlation should be used for those conditions.

Finally, just recall that only tested parameters are considered for fitting, however, there are others (such ambient turbulence) that may also affect *SSI*, *SoCF* and *LOL*. These non-controlled parameters would introduce an error in measurements. Nevertheless their relevance is negligible as demonstrated by the high values of R^2 obtained; the 98% of the change of *SSI*, *SoCF* and *LOL* is explained by the studied parameters.

5. Conclusions

Ignition delay and lift-off length have been studied in a wide range of Diesel relevant conditions using an ECN Diesel injector and a novel constant-pressure flow facility.

The measurements have been performed using ECN standard diagnostics (broadband and OH* chemiluminescence) accomplishing two objectives:

- To provide valuable experimental data for modelers that are consistent with ECN guidelines.
- To advance the understanding of the ECN experimental techniques testing over the whole range of parametric variation suggested.

The results remarked the very good repeatability of the diagnostics, finding a) good agreement with the literature and b) providing an accurate overall description of the relationship between

the measurements and the boundary conditions. These facts together can be considered as an important insight of the reliability of the data.

Moreover, a new processing method for Schlieren images allowed to characterize the onset of cool flames, and to obtain through a statistical analysis an analytical description that relates their timing with the boundary conditions.

Finally, a second parameter extracted by the Schlieren images processing (local maximum in the total intensity curve) has been compared to the *SSI* obtained via chemiluminescence. The good match between the two measurements suggests a strict link between the two phenomena observed, and the possibility to use the Schlieren imaging to measuring *SSI*. On the other hand, even if the absolute value of the measurements is always close, the statistical analysis shows that the effect of oxygen concentration and ambient density is caught differently by the two methodologies and therefore the reliability of this second technique could be questioned. However, the precise description of the ignition event provided by the Schlieren processing remains a useful tool and requiring only a relatively easy setup, being the results easy to reproduce in other facilities.

Acknowledgements

This work was sponsored by "*Ministerio de Economía y Competitividad*" of the Spanish Government in the frame of the Project "*Comprensión de la influencia de combustibles no convencionales en el proceso de injección y combustión tipo diesel*", Reference TRA2012-36932. Additionally, the Ph.D student Michele Bardi was financed by a grant from "*Conselleria de educacio, cultura y esport*" of the "*Generalitat Valenciana*" with Reference GRISOLIA/2010/010. This support is gratefully acknowledged by the authors.

The authors would also like to thank Juan Pablo Viera and José Enrique del Rey for their valuable work in the laboratory during the tests.

Bibliography

[1] R. Kiplimo, E. Tomita, N. Kawahara, and S. Yokobe, Effects of spray impingement, injection parameters, and EGR on the combustion and emission characteristics of a PCCI diesel engine, Applied Thermal Engineering 37 (2012) 165-175.

[2] R. Mobasheri, Z. Peng, and S. M. Mirsalim, Analysis the effect of advanced injection strategies on engine performance and pollutant emissions in a heavy duty DI-diesel engine by CFD modeling, International Journal of Heat and Fluid Flow 33 (2012) 59-69.

[3] J. I. Ramos, Internal Combustion Engine Modeling, Hemisphere Publishing Corporation, New York, United States of America, 1989.

[4] C. Hasse, V. Sohm, and B. Durst, Deatached eddy simulation of cyclic large scale fluctuations in a simplified engine setup, International Journal of Heat and Fluid Flow 30 (2009) 32-43.

[5] F. J. Salvador, J. Martínez-López, J. V. Romero, and M. D. Roselló, Influence of biofuels on the internal flow in diesel injector nozzles, Mathematical and Computer Modeling 54 (2010)

1699-1705.

[6] L. M. Pickett. (2012, February) Engine Combustion Network (ECN). [Online]. www.sandia.gov/ecn/ (last accessed on January 2013)

[7] M. Bardi et al., Engine Combustion Network (ECN): Comparison of Spray Development, Vaporizatin and Combustion in different Combustion Vessels, Atomization and Sprays 22 (2012) 807-842.

[8] R. Baert, P. Frijters, B. Somers, and C. Luitjen, Design and operation of a high pressure, high temperature cell for HD diesel spray diagnostics: guidelines and results, SAE Paper 2009-01-0649 (2009).

[9] D. L. Siebers and B. S. Higgins, Flame lift-off on direct-injection diesel sprays under quiescent conditions, SAE Paper 2001-01-0530 (2001).

[10] P. M. Lillo, L. M. Pickett, H. Pearson, O. Andersson, and S. Kook, Diesel spray ignition detection and spatial/temporal correction, SAE Paper 2012-01-1239 (2012).

[11] R. Payri, F. J. Salvador, J. Gimeno, and J. de la Morena, Effects of nozzle geometry on direct injection diesel engine combustion process, Applied Thermal Engineering 29 (2009) 2051-2060.

[12] L. M. Pickett, S. Kook, and T. C. Williams, Visualization of diesel spray penetration, cool-flame, ignition, high-temperature combustion, and soot formation using high-speed imaging, SAE Paper 2009-01-0658 (2009).

[13] L. Michalski, K. Eckersdorf, J. Kucharski, and J. McGhee, Temperature measurements, John Wiley & Sons Ltd., New York, United States of America, 2001.

[14] M. Meijer et al., Engine Combustion Network (ECN): Characterization and comparison of boundary conditions for different combustion vessels, Atomization and Sprays 22 (2012) 777-806.

[15] R. Payri, J. Gimeno, M. Bardi, and A. H. Plazas, Study Liquid Length penetration results with a Direct Acting Piezo Electric injector., Applied Energy (2013) doi:10.1016/j.apenergy.2013.010.027.

[16] R. Payri, J. M. Garcia-Oliver, M. Bardi, and J. Manin, Fuel temperature influence on diesel sprays in inert and reacting conditions, Applied Thermal Engineering 35 (2012) 185-195.

[17] A. L. Kastengren, F. Z. Tiloco, C. F. Powell, and R. Payri, Engine Combustion Network (ECN): Measurements of Nozzle Diameter and Hydraulic Behavior, Atomization and Sprays (2012) doi:10.1615/AtomizSpr.2013006309.

[18] L. M. Pickett et al., Comparison of diesel spray combustion in different high-temperature, high pressure facilities, SAE Paper 2010-01-2106 (2010).

[19] V. Macián, V. Bermúdez, R. Payri, and J. Gimeno, New technique for determination of internal geometry of a Diesel nozzle with the use of silicone methodology, Experimental Techniques 27 (2003) 39-43.

[20] A. G. Gaydon, The spectroscopy flames, Chapman & Hall, London, United Kingdom, 1974.

[21] J. E. Dec and E. B. Coy, Radical imaging in a direct Diesel engine and structure of the early diffusion flame, SAE Paper 960831 (1996).

[22] J. E. Dec and C. Espey, Chemiluminiscence Imaging of Autoignition in a Diesel Engine, SAE Paper 982685 (1998).

[23] R. Payri, F. Salvador, J. Gimeno, and J. de la Morena, Influence of injector technology and combustion development. Part 2: Combustion analysis, Applied Energy 88 (2011) 1130-1139.

[24] G. S. Settles, Schlieren and sadowgraph techniques: visualizing phenomena in transparent media (Experimental Fluid Mechanic), Springer Verlag, Heidelberg, Germany, 2001.

[25] R. Klein-Douwel, P. Fritjers, L. Somers, W. de Boer, and R. Baert, Macroscopic diesel fuel

spray shadowgraphy using high speed digital imaging in a high pressure cell, Fuel 86 (2007) 1994-2007.

[26] J. Naber and D. Siebers, Effects of gas density and vaporization on penetration and dispersion of diesel sprays, SAE Paper 960034 (1996).

[27] S. Parrish and R. Zink, Development and application of an imaging system to evaluate liquid and vapor envelopes of sprays from a multi-hole gasoline fuel injector operating under engine-like conditions, Atomization and Sprays 22 (2012) 647-661.

[28] R. Payri, J. Gimeno, J. Viera, and A. H. Plazas, Schlieren visualization for transient vapor penetration and spreading angle of a prototype diesel direct-acting piezoelectric injector, in ICLASS, Heidelberg, Germany, 2012.

[29] D. L. Siebers, Liquid-Phase Fuel Penetration in Diesel Sprays, SAE Internacional 980809 (1998).

[30] G. Shibata and H. Ogawa, HCCI Combustion Control by DME-Ethanol Binary Fuel and EGR, SAE International 2012-01-1577 (2012).

[31] S. Tanaka, F. Ayala, and J. C. Keck, A reduced chemical kinetic model for HCCI combustion of primary reference fuels in a rapid compression machine, Combustion and Flame 133 (2003) 467-481.

[32] R. H. Petrucci, F. Herring, J. D. Madura, and C. Bissonnette, General Chemistry: principles and modern applications, Pearson, Toronto, Canada, 2010.

[33] F. Pischinger, V. Reuter, and E. Scheid, Self-ignition of Diesel sprays and its dependence on fuel properties and injection parameters, Journal of Engineering for Gas Turbine and Power 110 (1988) 399-404.

[34] L. M. Pickett, D. L. Siebers, and C. Idicheira, Relationship between ignition processes and the lift-off length of diesel fuel jets, SAE Paper 2005-01-3843 (2005).

[35] R. Payri, F. J. Salvador, J. Gimeno, and V. Soare, Determination of diesel spray characteristics in real engine in-cylincer air density and pressure conditions, Journal of Mechanical Science and Technolgy 19 (2005) 2040-2052.

[36] I. V. Roisman, L. Araneo, and C. Tropea, Effect of ambient pressure on penetration of a diesel spray, International Journal of Multiphase Flow 33 (2007) 904-920.

APPLIED THERMAL ENGINEERING; Volume: 58; Issue: 1-2; Pages: 554-563;
DOI: 10.1016/j.applthermaleng.2013.04.044; Published: SEP 2013

List of figures

APPLIED THERMAL ENGINEERING; Volume: 58; Issue: 1-2; Pages: 554-563;
DOI: 10.1016/j.applthermaleng.2013.04.044; Published: SEP 2013

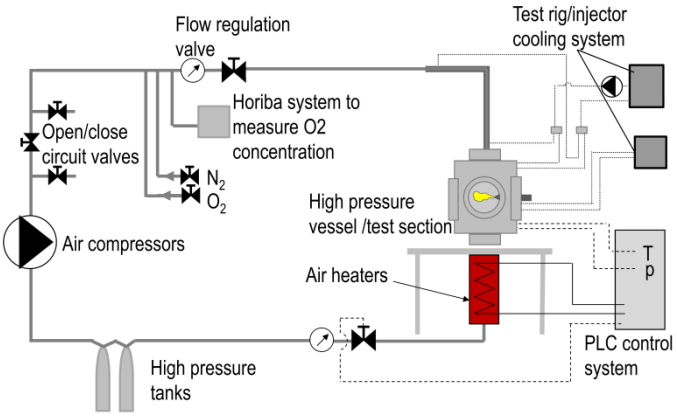

Fig 1

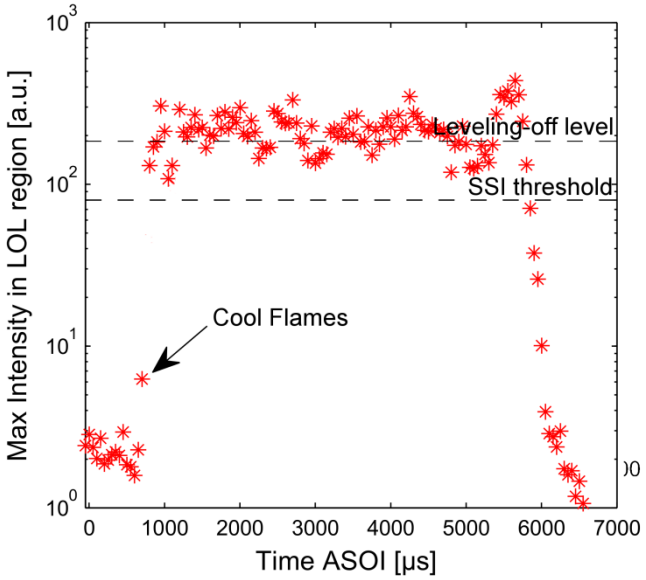

Fig 2

APPLIED THERMAL ENGINEERING; Volume: 58; Issue: 1-2; Pages: 554-563;
DOI: 10.1016/j.applthermaleng.2013.04.044; Published: SEP 2013

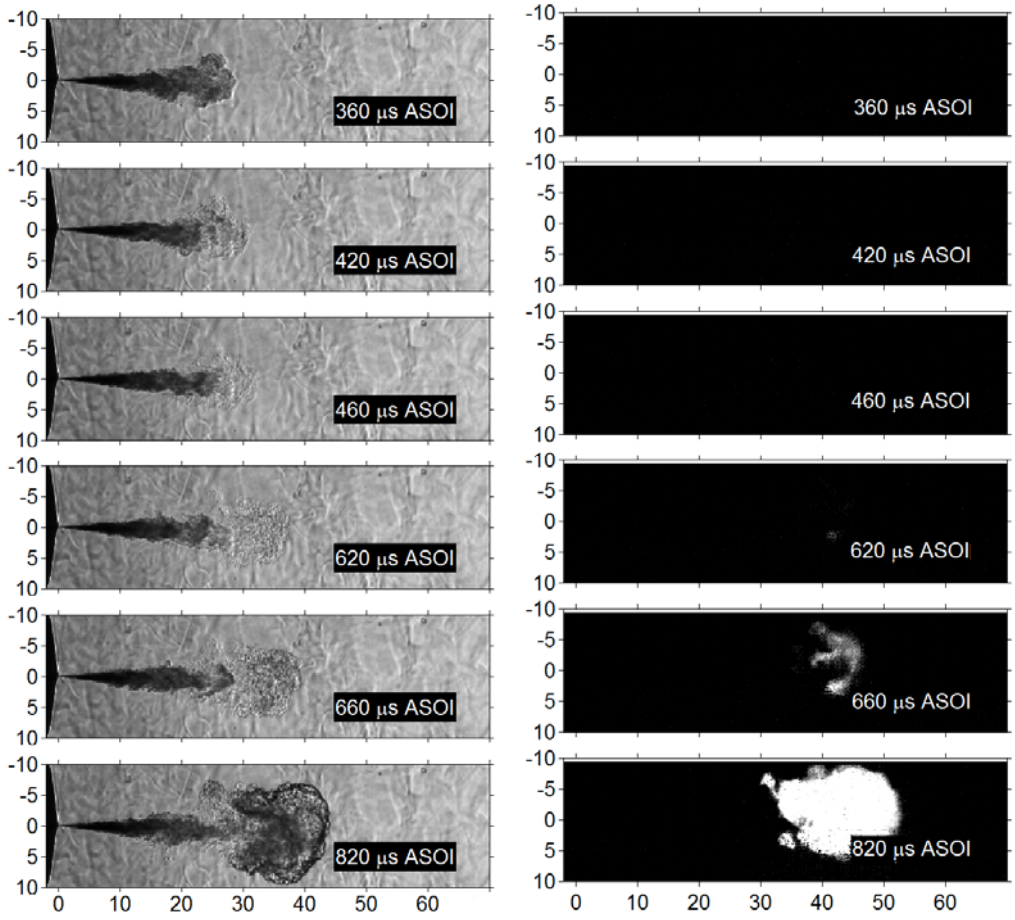

Fig 3

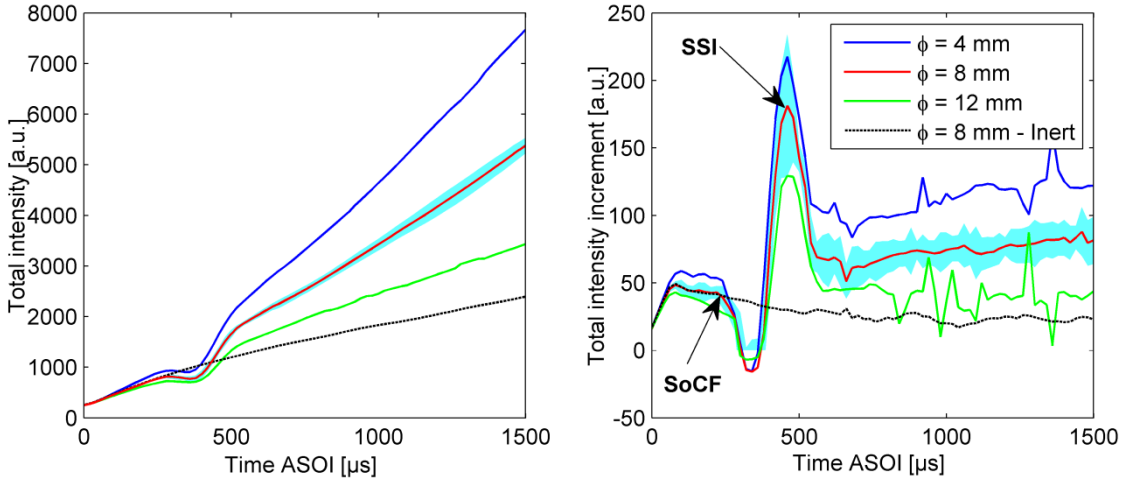

Fig 4

APPLIED THERMAL ENGINEERING; Volume: 58; Issue: 1-2; Pages: 554-563;
DOI: 10.1016/j.applthermaleng.2013.04.044; Published: SEP 2013

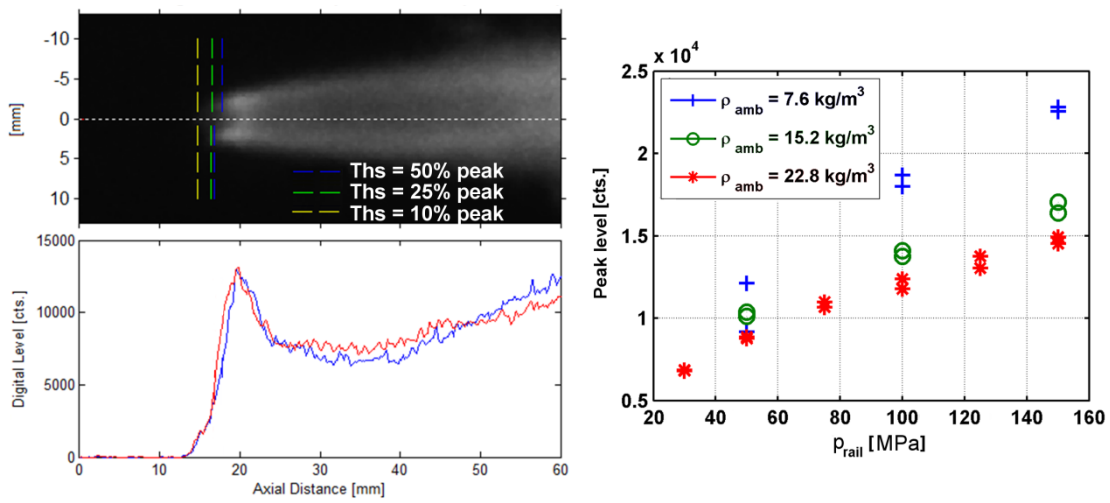

Fig 5

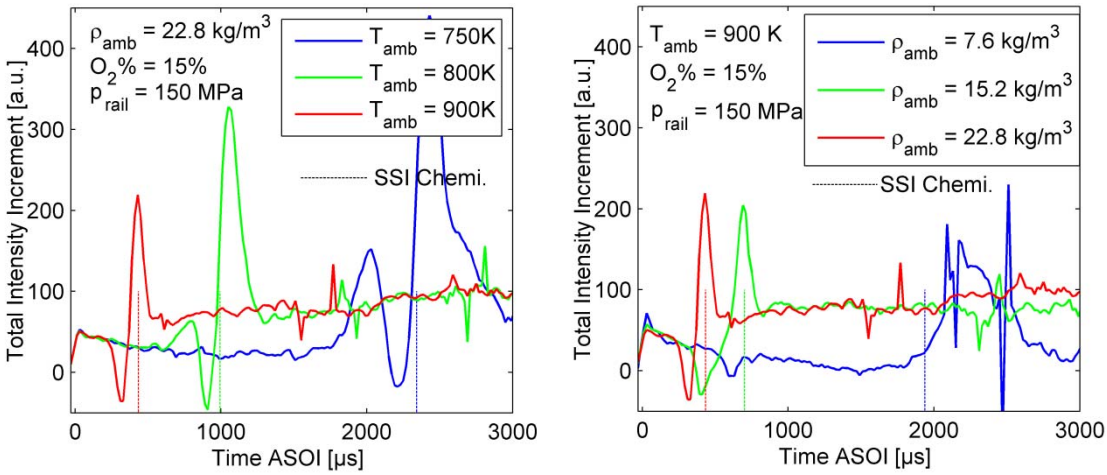

Fig 6

APPLIED THERMAL ENGINEERING; Volume: 58; Issue: 1-2; Pages: 554-563;
DOI: 10.1016/j.applthermaleng.2013.04.044; Published: SEP 2013

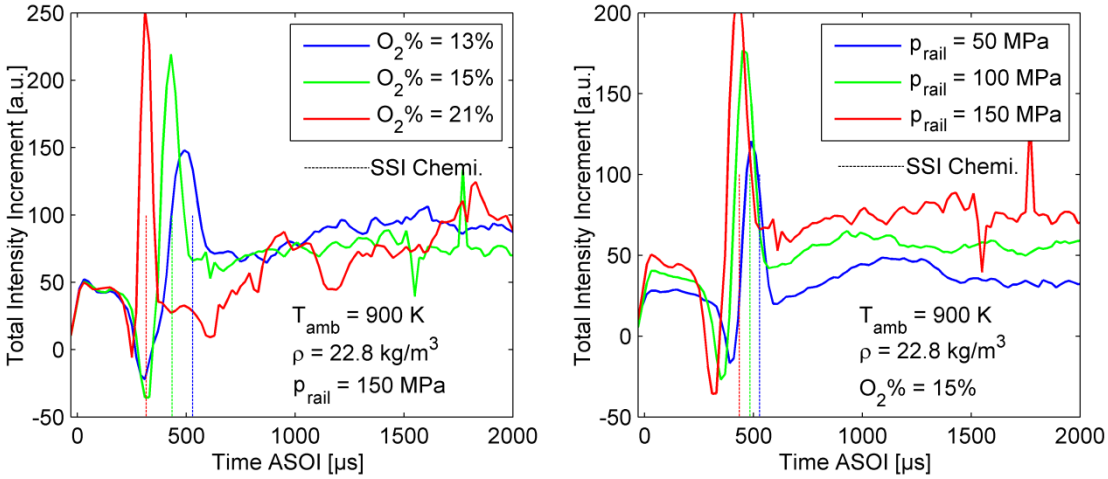

Fig 7

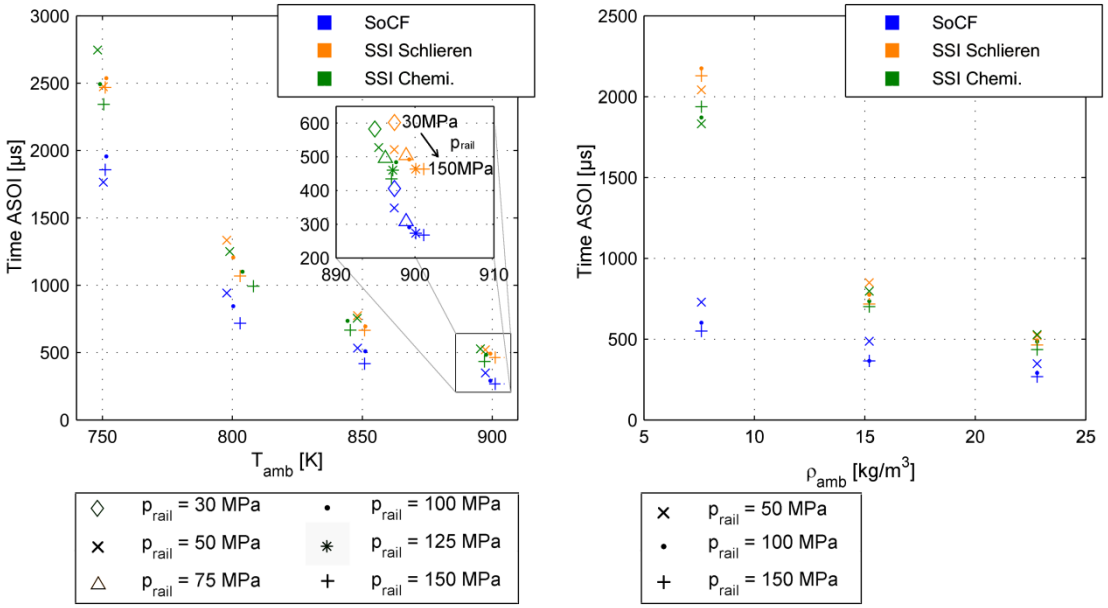

Fig 8

APPLIED THERMAL ENGINEERING; Volume: 58; Issue: 1-2; Pages: 554-563;
DOI: 10.1016/j.applthermaleng.2013.04.044; Published: SEP 2013

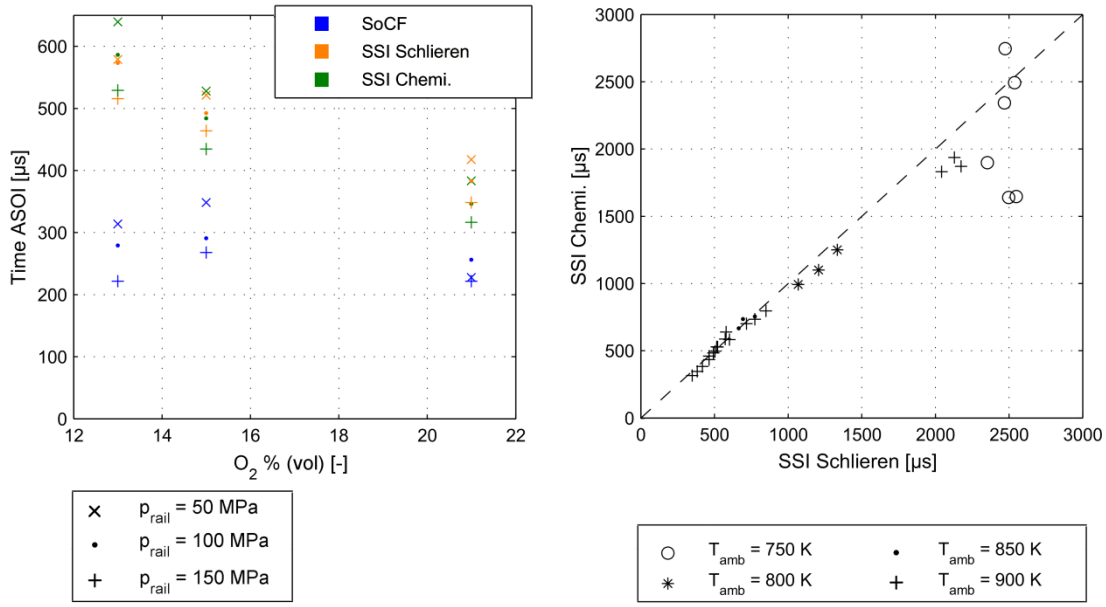

Fig 9

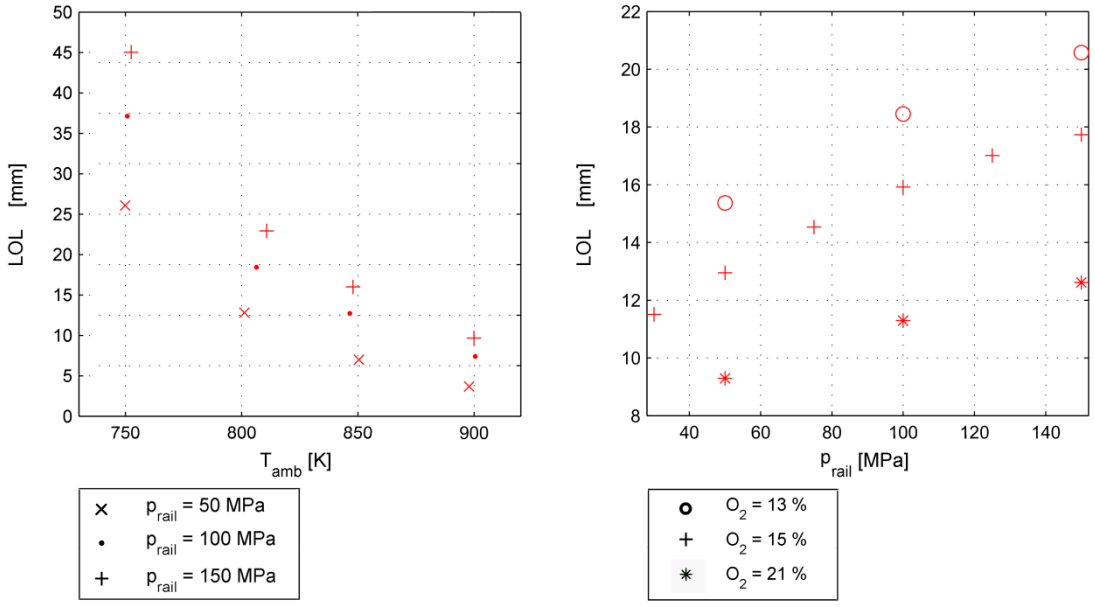

Fig 10

APPLIED THERMAL ENGINEERING; Volume: 58; Issue: 1-2; Pages: 554-563;
DOI: 10.1016/j.applthermaleng.2013.04.044; Published: SEP 2013

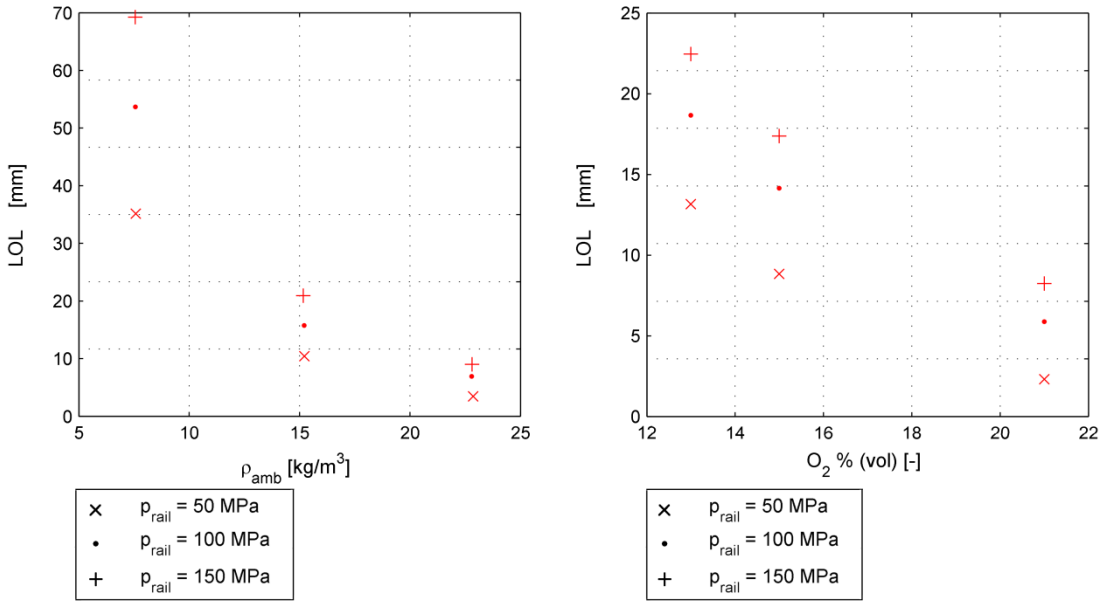

Fig 11

APPLIED THERMAL ENGINEERING; Volume: 58; Issue: 1-2; Pages: 554-563;
DOI: 10.1016/j.applthermaleng.2013.04.044; Published: SEP 2013